AFRL-RX-WP-TP-2010-4294

ELECTRONMAGNETIC CHARACTERIZATION OF CARBON NANOTUBE FILMS SUBJECT TO AN OXIDATIVE TREATMENT AT ELEVATED TEMPERATURE (Preprint)

John J. Boeckl, Angela L. Campbell, and Timothy L. Peterson

Electronic and Optical Materials Branch
Survivability and Sensor Materials Division

Richard A. Kleismit, Kineshma Munbodh, and Gregory Kozlowski

Wright State University

Krzysztof K. Koziol

University of Cambridge

JULY 2010
Interim Report

AIR FORCE RESEARCH LABORATORY
MATERIALS AND MANUFACTURING DIRECTORATE
WRIGHT-PATTERSON AIR FORCE BASE, OH 45433-7750
AIR FORCE MATERIEL COMMAND
UNITED STATES AIR FORCE

REPORT DOCUMENTATION PAGE

Form Approved
OMB No. 0704-0188

1. REPORT DATE *(DD-MM-YY)*	2. REPORT TYPE	3. DATES COVERED *(From - To)*
July 2010	Journal Article Preprint	27 January 2006 – 26 June 2010

4. TITLE AND SUBTITLE

ELECTRONMAGNETIC CHARACTERIZATION OF CARBON NANOTUBE FILMS SUBJECT TO AN OXIDATIVE TREATMENT AT ELEVATED TEMPERATURE (Preprint)

5a. CONTRACT NUMBER
IN-HOUSE

5b. GRANT NUMBER

5c. PROGRAM ELEMENT NUMBER
62102F

6. AUTHOR(S)

John J. Boeckl, Angela L. Campbell, and Timothy L. Peterson (Survivability and Sensor Materials Division, Electronic and Optical Materials Branch (AFRL/RXPS))
Richard A. Kleismit, Kineshma Munbodh, and Gregory Kozlowski (Wright State University)
Krzysztof K. Koziol (University of Cambridge)

5d. PROJECT NUMBER
4348

5e. TASK NUMBER
RG

5f. WORK UNIT NUMBER
M07R5000

7. PERFORMING ORGANIZATION NAME(S) AND ADDRESS(ES)

Electronic and Optical Materials Branch
Survivability and Sensor Materials Division
Materials and Manufacturing Directorate
Wright-Patterson Air Force Base, OH 45433-7750
Air Force Materiel Command, United States Air Force

Wright State University
Physics Department

University of Cambridge
Department of Materials Science and Metallurgy

8. PERFORMING ORGANIZATION REPORT NUMBER
AFRL-RX-WP-TP-2010-4294

9. SPONSORING/MONITORING AGENCY NAME(S) AND ADDRESS(ES)

Air Force Research Laboratory
Materials and Manufacturing Directorate
Wright-Patterson Air Force Base, OH 45433-7750
Air Force Materiel Command
United States Air Force

10. SPONSORING/MONITORING AGENCY ACRONYM(S)
AFRL/RXPS

11. SPONSORING/MONITORING AGENCY REPORT NUMBER(S)
AFRL-RX-WP-TP-2010-4294

12. DISTRIBUTION/AVAILABILITY STATEMENT
Approved for public release; distribution unlimited.

13. SUPPLEMENTARY NOTES
PAO case number 88ABW-2010-3440, cleared 22 June 2010. The U.S. Government is joint author of this work and has the right to use, modify, reproduce, release, perform, display, or disclose the work. To be published in Journal Nanosci. Nanotechnol., 2009 Aug;9(8):4543-53. Document contains color.

14. ABSTRACT

Electromagnetic characterization of carbon nanotube (CNT) films fabricated by thermal decomposition of silicon carbide (SiC) has been performed. Purification and/or uncapping treatment conditions at an elevated temperature of 400 °C under flowing oxygen or carbon dioxide have been studied. A near field microwave microscope was used to measure the real and imaginary parts of the complex permittivity of CNT films through the frequency shift and the change in reciprocal quality factor between two extreme positions of an evanescent microwave probe-tip (in contact with the sample, and away from interaction with it). A theoretical two-point model was proposed to confirm experimental data, which showed poor conductivity of the CNT film as grown but has slight improvement after 40-minute treatment.

15. SUBJECT TERMS
evanescent microwave microscopy, permittivity, quality factor, purification and uncapping of carbon nanotubes

16. SECURITY CLASSIFICATION OF:			17. LIMITATION OF ABSTRACT:	18. NUMBER OF PAGES	19a. NAME OF RESPONSIBLE PERSON (Monitor)
a. REPORT	b. ABSTRACT	c. THIS PAGE			Charles Stutz
Unclassified	Unclassified	Unclassified	SAR	32	19b. TELEPHONE NUMBER *(Include Area Code)* N/A

Standard Form 298 (Rev. 8-98)
Prescribed by ANSI Std. Z39-18

Electromagnetic characterization of carbon nanotube films subject to an oxidative treatment at elevated temperature

Richard A. Kleismit[1], Kineshma Munbodh[1], John J. Boeckl[2], Angela L. Campbell[2], Krzysztof K. Koziol[3], Gregory Kozlowski[1,3], Simon C. Hopkins[3], and Timothy L. Peterson[2]

[1] Physics Department, Wright State University, Dayton, OH 45435, U.S.A.
[2] Materials and Manufacturing Directorate, Air Force Research Laboratory, Wright-Patterson AFB, OH 45433, U.S.A.
[3] Department of Materials Science and Metallurgy, University of Cambridge, Pembroke Street, Cambridge, CB2 3QZ, UK

E-mail: gregory.kozlowski@wright.edu

ABSTRACT

Electromagnetic characterization of CNT films fabricated by thermal decomposition of SiC has been performed. Purification and/or uncapping treatment conditions at an elevated temperature of 400°C under flowing oxygen or carbon dioxide have been studied. A near field microwave microscope was used to measure the real and imaginary parts of the complex permittivity of CNT films through the frequency shift and the change in reciprocal quality factor between two extreme positions of an evanescent

microwave probe-tip (in contact with the sample, and away from interaction with it). A theoretical two-point model was proposed to confirm experimental data, which showed poor conductivity of the CNT film as grown but has slight improvement after 40 min treatment.

Key words: evanescent microwave microscopy, permittivity, quality factor, purification and uncapping of carbon nanotubes

INTRODUCTION

Carbon nanotubes (CNTs) have attracted a lot of attention since their discovery in 1991 by Iijima [1]. They are used in a variety of applications from nanoelectronics through microwave amplification to sensors. Assemblies of nanotubes in the form of films or carpets can be used as flat panel displays or lighting elements (e.g., the brightness of CNT arrays is higher by a factor of two than conventional thermionic lighting elements for giant outdoor displays). CNTs grown by arc-discharge, laser ablation and chemical vapor deposition (CVD) can appear in a large variety of forms [2]-[4]. Single-walled nanotubes (SWNTs) have a mean diameter of one nanometer, lengths that can reach several microns, and end in a spherical cap. The lengths of multi-walled nanotubes (MWNTs) are usually well over 10 μm with diameters up to 70 nm [5]-[18], and they show tips with a polyhedral shape. Finally, nanotubes produced by catalytic reactions often show partially ordered layers containing extended structural defects. The relatively small diameter of CNTs is very favorable for field emitters, devices based on the process by which a substance emits electrons when an electric field or voltage is applied to it. The electric field has to be very high, in the order of 10^7 V/cm. To reach this value, the field amplification effect is very helpful: namely, the electric field lines are concentrated more densely around a sharp object (e.g., the tip of the CNTs). Nanotubes ensure very high field amplification because of their elongated shape. The maximum current drawn from one single-walled nanotube is ~ 0.2 mA and from multi-walled nanotube ~ 0.1 mA. It appears that open tubes are far less efficient emitters than closed ones: the voltage needed for emission is typically a factor of two higher for open

nanotubes. This is a surprising result since the smaller effective curvature of the open nanotubes was expected to lead to larger field amplification. However, it is now thought that oxygen atoms attract themselves to the free dangling bond at the ends of the nanotube, resulting in localized electron states. Since these states lie well below the Fermi energy in the nanotube, they cannot emit electrons. Localized states are formed also at the tips of closed nanotubes but these states are coupled to π-orbitals, effectively enhancing the emission of electrons [13]. Useful parameters for a comparison of the field emission performances of the different types of nanotube are the turn-on field (ranging from 0.4 V/μm to 7.5 V/μm) and the threshold field (from 0.9 V/μm up), i.e., the electric fields needed to produce current densities of 10 $\mu A/cm^2$ and 10 mA/cm^2, respectively [9]-[13].

For multi-stage carbon nanotube emitters grown on porous silicon by the CVD method (the average length and diameter of the SWNTs and thin MWNTs were ~ 10 μm – 15 μm and ~ 2 nm – 10 nm, respectively) the turn-on field and current at a field of 1 V/μm were ~ 0.4 V/μm, 0.6 V/μm and ~ 450 μA, 14 μA, respectively [15].

Liu et al. [17] reported field emission measurements on CNTs grown on silicon nanowire arrays by the CVD method, with turn-on field and threshold field respectively equal to 2.3 V/μm and 3.2 V/μm. The voltages needed for a given emission current are typically a factor of two higher for open tubes: the voltage increased from 190 V to 400 V, and from 320 V to 570 V, for 10 nA and 10 A emission, respectively.

There is a significant difference in the field emission characteristics between single-walled, closed and open arc-discharge multi-walled, and catalytically grown multi-walled nanotubes. To obtain low operating voltages as well as long emitter lifetimes, the nanotubes should be multi-walled and have closed, well graphitized tips. The optimal emitters are thus closed arc-grown MWNTs. SWNTs degrade substantially faster, as do MWNTs with disordered structures, in addition to requiring high voltages for emission. Finally, the emission performance of MWNT nanotubes is seriously degraded by opening their ends.

Nanotube films (carpets) display the lowest emission voltage for closed MWNT films, followed by closed SWNTs, opened MWNTs and SWNTs. A much more

homogeneous emission image is obtained for a medium-density nanotube film primarily due to the large number of emitting sites involved and above all the smaller screening effects. One of the factors for efficient field emission is the distance between CNTs, which should be greater than their height to minimize the electric field screening effect [18]. Taking into account the appropriate lengths of the tubes and the distances between neighboring emitters, sufficient field amplification can be reached in these films. To obtain low operating voltages as well as long emitter lifetimes, the CNT films should be multi-walled and have closed, well-ordered tips.

The field emission behavior of carbon nanotubes cannot be understood solely by assuming emission from metallic tips. The luminescence and measurements of the energy distribution of the emitted electrons indicate that the electrons are emitted from states in a narrow band of ~ 0.3 eV half-width. In fact, theoretical calculations show that the local density of states at the tip presents sharp localized states that are correlated to the presence of pentagonal defects [13]. The observed luminescence strongly suggests that although the greatest part of the emitted current comes from occupied states with a large density of states near the Fermi level, other, deeper levels also contribute to the field emission. The position of the tip states with respect to the Fermi level influences directly the field emission properties of the tube. Indeed, only tubes with a band state just under or over the Fermi level are good candidates for field emission.

This partially non-metallic character of the emission suggests that, at and above room temperature, the body of a carbon nanotube behaves essentially as a graphitic cylinder. This means that the carrier density at the Fermi level is very low, on the order of $5 \cdot 10^{18}$ cm^{-3}, which is three orders of magnitude lower than for a metal. Simulations show that the local density of states at the tip reaches values at least 30 times higher than in the cylindrical part of the tube. Since the field emission depends directly on this carrier density, the field emission current would be far lower without these localized states for a geometrically identical tip. The superiority of closed MWNTs over the other types is in this respect an additional indication, since the position and intensity of the localized states are strongly influenced by the crystalline structure. A disordered or, worse, missing tip would consequently lead to inferior performance as was observed for open and catalytically-grown MWNTs [14]. Well-aligned and randomly grown MWNTs

fabricated by the radio-field-induced self-bias hot-filament on silicon and Ni-Fe alloys by the CVD method were used for field emission applications by Chen et al. [16]. It was suggested in [16] that the dominant contribution to the field emission comes from amorphous carbon at the sharp tip of the CNTs, which have a high aspect ratio, and was attributed to thermal electrons escaping over the Schottky barrier at the interface between the metallic carbon MWNTs and the semiconducting amorphous carbon caps and tunneling into the vacuum. A large hysteresis between the rising and falling I –V sweeps has been observed by Liu et al. [17], indicating the influence that absorbates on CNT tips can have on field emission: when absorbates are removed the emission currents are lower during the downwards voltage ramp.

The reactivity of CNTs makes them attractive host materials for storage of neutral species and electron donors. There is a fine line between emission application of carbon nanotubes, which requires carbon nanotubes to be purifed and capped, and storage application, where nanotubes should be purified and uncapped. It appears that both (purification and uncapping) can be done at the same time by annealing. The simplest method to open the nanotubes is by oxidative treatment. It is well known that graphite oxidizes primarily at defects of the hexagonal lattice to create etch pits. When such defect sites are present in the wall of nanotubes, they become centers of preferential etching. However, nanotubes have additional structural features such as high curvature, helicity and contain five or seven-membered rings which modify the initiation and propagation of oxidation. Ajayan et al. [22] etched away carbon nanotube caps by oxidizing them in air for short durations: above 700°C samples showed a substantial weight loss and they entirely disappeared when heated for 15 minutes at 850°C. Tsang et al. [23] reported that heating multi-walled carbon nanotubes in carbon dioxide gas resulted in the partial or complete destruction of the tube caps and/or stripping of the outer layers to produce thinner tubes. The material was heated under a flow of 20 ml/min carbon dioxide gas at 850°C for 5 h. These open tubes were regarded as nanoscale test-tubes for adsorption of other molecules. The selective reaction of the gas with the curved part of a cap reflects greater reactivity, which may be due to greater strain and the presence of pentagonal rings.

In order to remove amorphous carbon catalyst-free material can either be oxidized or reduced [24]. Reduction is usually performed in a hydrogen atmosphere above 700°C: oxidation can be performed either in the gas or the liquid phase. Gas phase oxidation is performed at 500°C in air and a 4 h treatment can achieve purity higher than 95 %: oxygen or ozone can also be used. When purification is carried out in solution, the use of an acidic (0.5 M sulfuric acid) $KMnO_4$ solution (0.3 M) is recommended. After one hour reaction at 80°C, carbon nanotubes of 95 % purity can be obtained. In some instances these treatments lead to uncapping of nanotubes. Geng et al. [25] have shown that the surfaces of SWNT bundles synthesized by laser ablation after vacuum annealing at 400°C for 10 h have much less amorphous carbon. A process for purifying carbon impurities and uncapping carbon nanotubes in the temperature range between about 120°C to about 180°C with a reagent selected from the group consisting of liquid phase oxidation agents, liquid phase nitration agents and liquid phase sulfonation agents was published in [26].

In all the fabrication techniques mentioned above magnetic nanoparticles were used as catalysts and they had to be removed at the end of the process. The purification techniques involved in the removal of magnetic impurities are usually tedious, expensive and cause degradation of the CNTs. In 1999, Kusunoki et al. [19]-[20] discovered a new and catalyst-free method for the growth of CNTs: surface decomposition of silicon carbide (SiC). This thermal decomposition of a SiC surface (either a carbon or a silicon face) under vacuum from 10^{-3} Torr to 10^{-7} Torr and at temperatures ranging from 1400 °C to 1700 °C yields a thin film of metal-free carbon nanotubes [21]. The resulting array or film of well-aligned CNTs allows for more accurate determination of their electromagnetic properties, especially their local and reduced complex permittivity ($\varepsilon_1 - i\varepsilon_2$).

Localized measurements at microwave frequencies (~ 1 GHz) are primarily motivated by the need for the characterization and quality assurance of materials. To reveal spatially-resolved dielectric properties and microstructural effects in materials, a scanning evanescent microwave microscope has been used (for a detailed description of the apparatus, see our previous publications [26]-[27]). In performing quantitative measurements of electromagnetic properties, the detailed electrostatic field configuration outside the tip is required. The probe tip and sample must be considered as a whole, and

the solution of the electrostatic field equations at real boundary conditions and practical limits must be adhered to in obtaining the perturbed field distributions. This will generate a methodology that explicitly relates the tip-sample distance to the relative resonant frequency shift of the resonator $\Delta f/f$, the change of the reciprocal quality factor $\Delta(1/Q)$ and physical material properties for a given probe geometry.

The main objective of our paper is to study purification (mainly the removal of amorphous carbon) and/or uncapping of CNT films synthesized by catalyst-free surface decomposition of silicon carbide, and to measure their local surface permittivity using the evanescent microwave microscope. Using our theoretical two-point model [29], obtaining the local permittivity requires measurements of only two extreme values of the frequency and quality factor: one pair, f_0 and Q_0, when the tip is well separated from the sample (not interacting with the film) and another pair, f and Q, when the tip touches the film surface. Our model relates the changes $\Delta f/f$ and $\Delta(1/Q)$ between these two positions to the real and imaginary parts ε_1 and ε_2 of the relative dielectric constant. We will evaluate the relative complex permittivity of carbon nanotube films formed by SiC thermal decomposition subjected to oxidative treatment in an oxygen or carbon dioxide atmosphere at 400°C. Additionally, Q-factor mapping over the CNTs surface will provide important information about changes in the conductive properties of the films subjected to the oxidative treatment.

EXPERIMENTAL

Commercial grade 6H and 4H silicon carbide (n-type, 8° off-axis wafers, Cree Inc.) were used to grow carbon nanotube films. They were cleaned by the standard RCA cleaning process [21]. These clean silicon carbide substrates were then placed in a graphite resistance furnace (Oxy-Gon Industries, Inc., Epsom, NH) at a temperature between 1400°C and 1700°C for 0.5 h - 12 h with a moderate vacuum pressure between 10^{-3} Torr and 10^{-5} Torr produced by a turbomolecular pump [21]. The furnace was double-walled and electropolished for high vacuum quality, and incorporated ports for visual observation, thermocouples and gas inflow. The samples were prepared at

1700°C and under a pressure of 10^{-4} Torr are shown in Tab.I.

A typical continuous film of vertically aligned carbon nanotubes with a thickness of 250 nm was obtained for the carbon-faced sample heated for 1 h at 1700°C. The CNTs were both single- and multi-walled (SWNTs and MWNTs). The nanotube diameter decreases with height and is wider at the interface between the SiC substrate and the CNT film. Amorphous carbon and a small amount of oxygen were also detected in the CNT films by X-ray photoelectron spectroscopy (XPS) [28]. The amorphous carbon is the residual carbon left on the surface of the carbon nanotubes after the sublimation of silicon from the surface of silicon carbide. As measured by Energy Despersive X-ray Spectroscopy (EDS) on the transmission electron microscopy (TEM) samples, the resulting CNT films contained less than 1% by weight of silicon. The CNTs formed from the crystalline substrate were well-aligned and straight as shown in Fig.1. This typical cross-section transmission electron micrograph was obtained by using a Philips CM-200 field emission gun (FEG) TEM operated at 200 kV. Fig.2 shows a typical topographical AFM image of the CNT film obtained by using the tapping mode (Veeco multimode V AFM/SPM).

The length of the CNTs increased almost linearly with growth time at 1700°C, reaching approximately 300 nm on the silicon face and 500 nm on the carbon face for a 6 h growth time [21]. The rate of formation of CNTs on the carbon face of the silicon carbide substrate is 1.7 times that on the silicon face. This difference in formation rates could be explained by differences in surface preparation and/or the presence of a thin oxide layer on the silicon-terminated face.

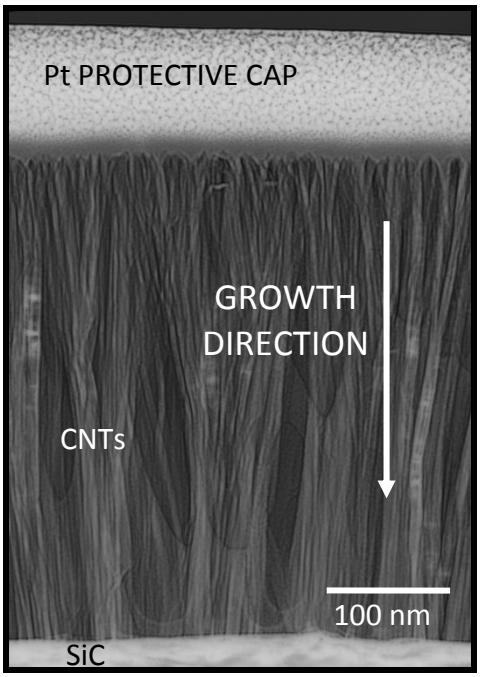

Fig.1. A typical very dense film of aligned CNTs attached to the SiC substrate (Si-face, 3 h).

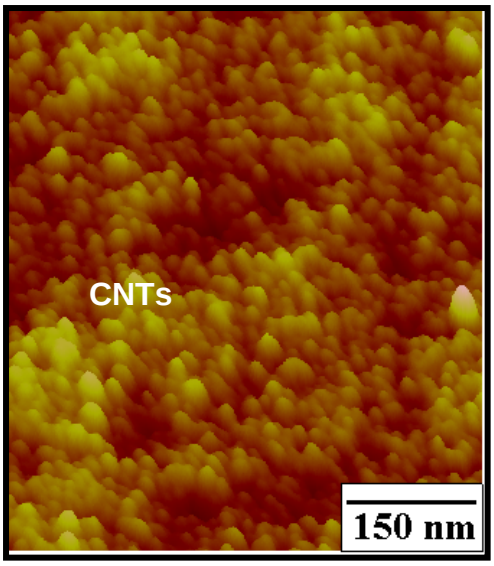

Fig.2. A typical topographical AFM image of the CNT film (Si-face, 3 h).

TAB.I. LIST OF CNT FILMS FABRICATED BY THE SURFACE DECOMPOSITION METHOD.

CNT FILMS	GROWTH TIME (h)	QUANTITY
C-face	1	3
Si-face	1	3
C-face	3	2
Si-face	3	4
C-face	6	3
Si-face	6	2

The post-growth treatment of the CNT films was carried out by placing the sample in a box furnace at 400°C under flowing oxygen or carbon dioxide. We also verified that a higher temperature could be used to obtain the same results in a shorter time. A type 30400 box furnace with a programmable Thermolyne temperature controller with four electric resistive heaters embedded in ceramic fiber refractory insulation was used for the post-growth treatment. The temperature was ramped to 400°C within 1 hour in the initial pre-heating stage of our experiment. The temperature in the box furnace was measured using a K-type thermocouple and an additional thermocouple near the sample holder was used to monitor the sample temperature. The measured furnace and sample temperatures were in good agreement (within ± 5°C). A gas deflector was also used to ensure that the gas would be directed towards the sample. The sample was inserted into the furnace when the temperature was 400°C ± 5°C, typically falling to 380°C when the door of the furnace was opened and recovering within 3 minutes. The samples were kept in the furnace for 25 min, 40 min or 60 min under flowing oxygen or carbon dioxide at this temperature, after which the door was slightly opened and the CNTs were allowed to cool slowly under oxygen or carbon dioxide. The samples were removed after 1 hour from the furnace when the temperatures on both

meters were 100°C and Tab.II shows the list of the samples which we were chosen for the demonstration of the purification/uncapping procedure.

TAB.II. POST-GROWTH TREATMENT OF CNT FILMS.

CNT FILM	DWELLING TIME (min) at 400°C	OXIDATIVE TREATMENT
Si-face (3 h)	25	O_2
	40	
	60	
Si-face (6 h)	25	CO_2
	40	
	60	

STRUCTURAL AND CHEMICAL CHARACTERIZATION

After each step of the purification/uncapping procedure, before and after the annealing process, our samples were subjected to structural, chemical and physical analyses. SEM, TEM, AFM, XRD, EDS and evanescent microwave measurements were carried out for the samples listed in Tab.II.

A Transmission Electron Microscope/Electron Diffraction Spectroscopy (TEM/EDS) system was used to determine the percentage composition of silicon and carbon in the SiC wafer before and after growth of the CNT to compare the change in the composition of the sample. Fig.3 shows the EDS spectrum.

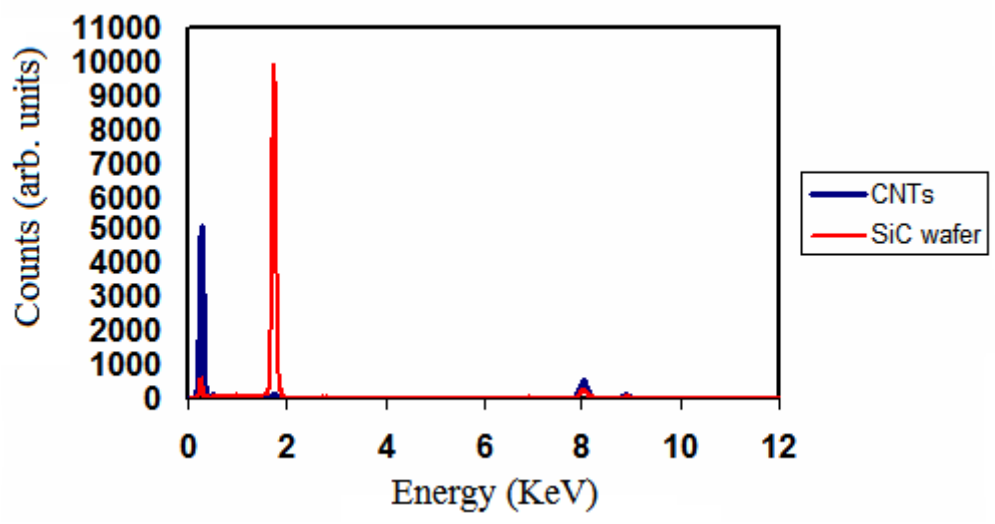

Fig.3. EDS spectrum of the SiC wafer before and after the growth of the CNT.

The quantitative percentage composition of the wafer before and after the growth of the CNT is shown in Tab.III.

TAB.III. COMPOSITION OF UNTREATED SiC SAMPLE (a) AND AFTER GROWTH OF CNT FILM (b).

Quantitative for SiC bulk		
Element	Wt %	Atom %
Si-K	63.08	42.21
C-K	36.92	57.79

(a)

Quantitative for CNT layer		
Element	Wt %	Atom %
Si-K	0.17	0.07
C-K	99.83	99.93

(b)

The data show that the untreated silicon carbide sample has 63.08 % of silicon and 36.92 % of carbon by weight. After growth of CNTs, the weight of silicon decreased to 0.17 % and the carbon increased to 99.83 %, indicating that most of the SiC decomposes to form CNT. SEM analysis showed the presence of white areas on the surface of the silicon face before the annealing treatment. The white spots in the image

are due to amorphous carbon, which is formed on the sample surface during the annealing temperature ramp up and cool down in the presence of oxygen.

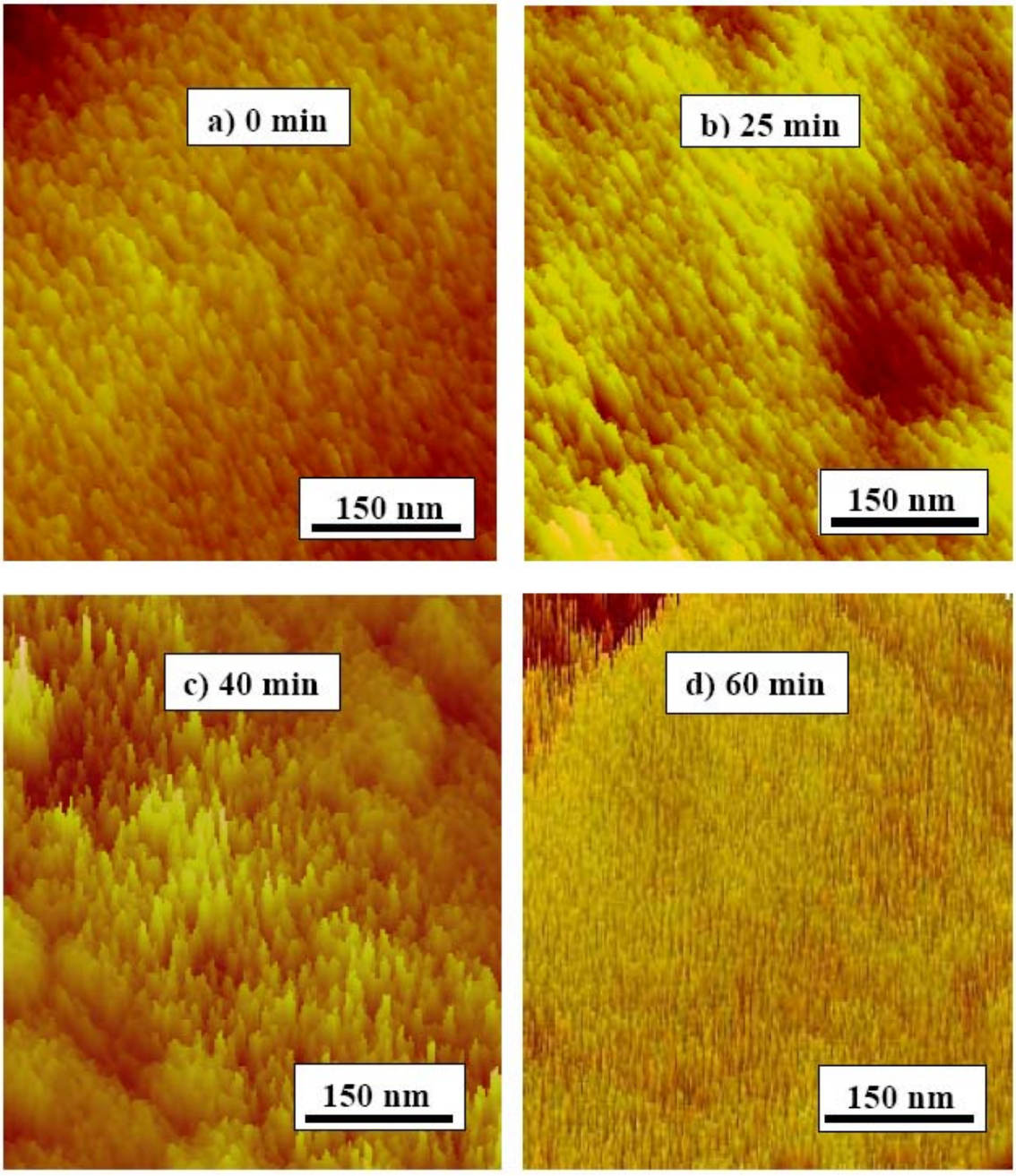

Fig.4. Typical AFM images of surface potential for Si-face (3 h) CNT film (a) as grown and after (b) 25 min, (c) 40 min and (d) 60 min annealing treatment in oxygen at 400°C.

Typical AFM surface potential micrographs are presented in Fig.4 for Si-face (3 h) CNT films as grown (a) and with purification/uncapping annealing treatment at 400°C

after 25 min (b), 40 min (c) and 60 min (d) dwelling time. A near field evanescent microwave microscopy sensor was used to characterize the CNT films through frequency shift measurements. The relative sensitivity of the microscope is in the range of 10^{-2} and the resolution is governed by the radius of the probe-tip [26]. The microwave probe consists of a tuned $\lambda/4$ coaxial transmission line with an end wall aperture. A transverse electromagnetic wave created by a frequency generator moves along the coaxial probe and is totally internally reflected at the surface of the end wall aperture. The evanescent waves emanate from a sharpened tip extending concentrically through the aperture and interact with the sample. The coaxial microwave probe is capacitively coupled to the sample, and to a network analyzer through a tuning network.

The probe can be operated in two different modes:

(1) Local complex permittivity determination by measuring the quality factor and resonant frequency shift as the tip approaches the sample. The resonant frequency data are produced by setting the reference resonant frequency at approximately 10 μm above the sample surface and moving the probe tip in micrometer steps to a distance of 1 μm from the surface. The resonant frequency shift data is best fitted by a method of images model that produces the real and complex part of permittivity [26].

(2) X-Y scanning of material properties, with a constant separation between tip and sample. Changes in the probe's resonant frequency, quality factor and reflection coefficient are tracked by a Hewlett-Packard 8722ES network analyzer as the probe is moved relative to the sample using an X-Y stage driven by optically encoded, dc and linear actuators. The probe is frame mounted to a Z-axis linear actuator assembly and the probe-sample separation can be set precisely.

The X-Y stage actuators, network analyzer and the data acquisition are computer controlled with National Instruments Labview® software. The complete evanescent microwave scanning system is mounted on a vibration-damping table.

Typical experimental data for the resonant frequency and the quality factor as a function of the tip-sample separation are plotted in Figs.5 and 6 respectively, for a CNT film (Si-face) grown for 3 h.

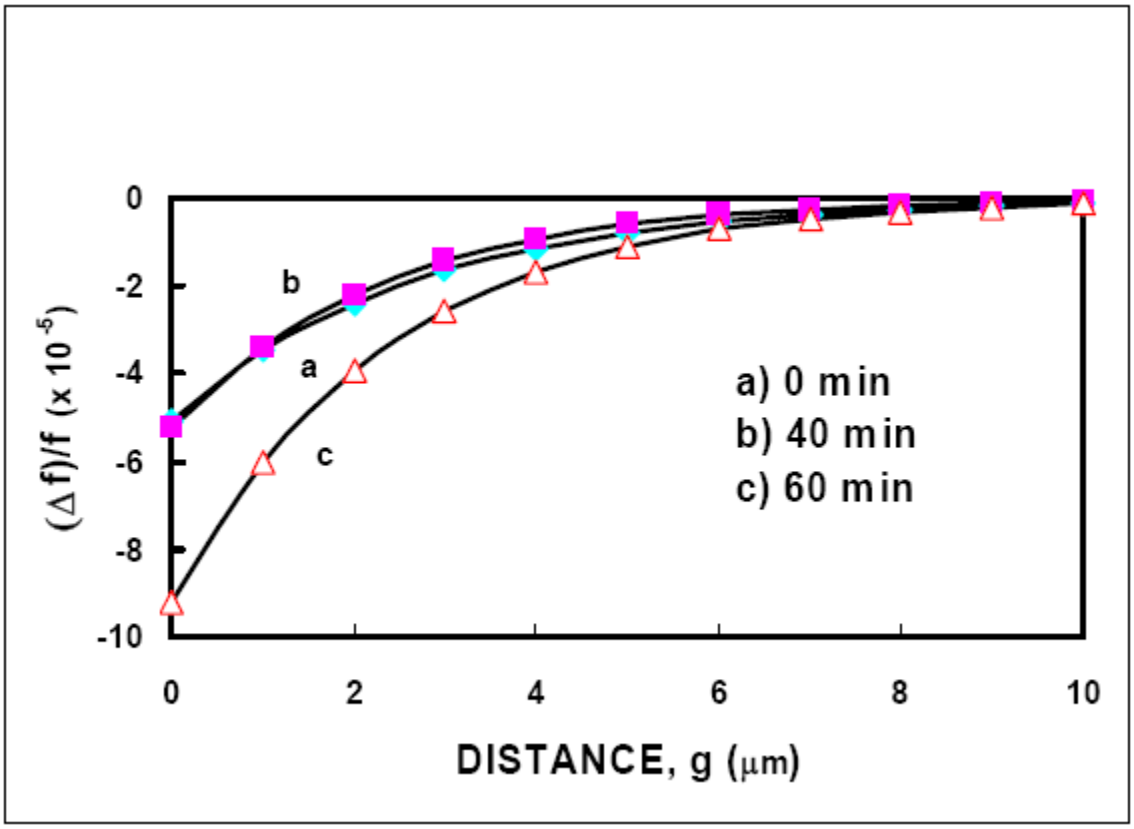

Fig.5. Experimental data points and theoretical fitting curves of relative resonant frequency change as a function of distance for Si-face (3 h) CNT film as grown (a) and after 40 min (b) and 60 min (c) annealing treatment in oxygen at 400°C.

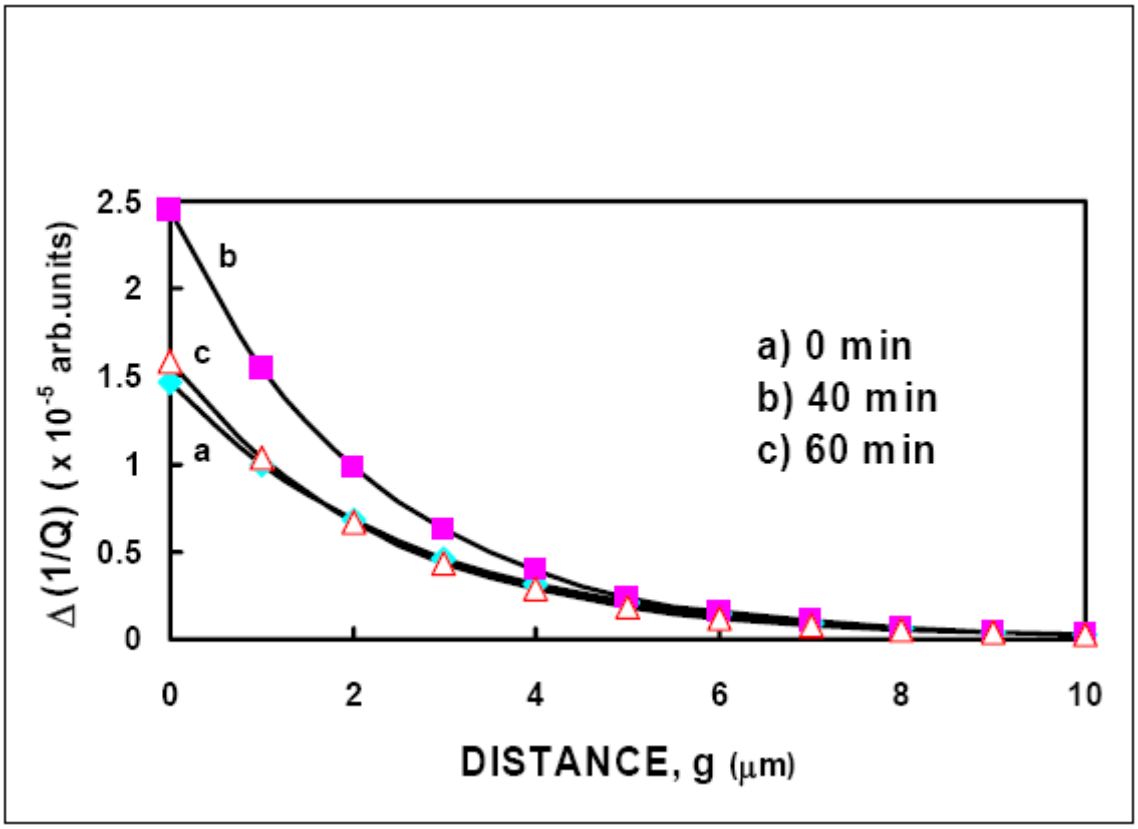

Fig.6. Experimental data points and theoretical fitting curves of reciprocal change of quality factor as a function of distance for Si-face (3 h) CNT film as grown (a) and after 40 min (b) and 60 min (c) annealing time in oxygen at 400°C.

The surface conductivities of CNT films (Si-face) grown for 3 h and 6 h were mapped over an area of 100 μm x 100 μm before and after the annealing treatments of 25 min, 40 min and 60 min in O_2 and CO_2 flowing gas, and they are shown in Figs.7 and 8 respectively.

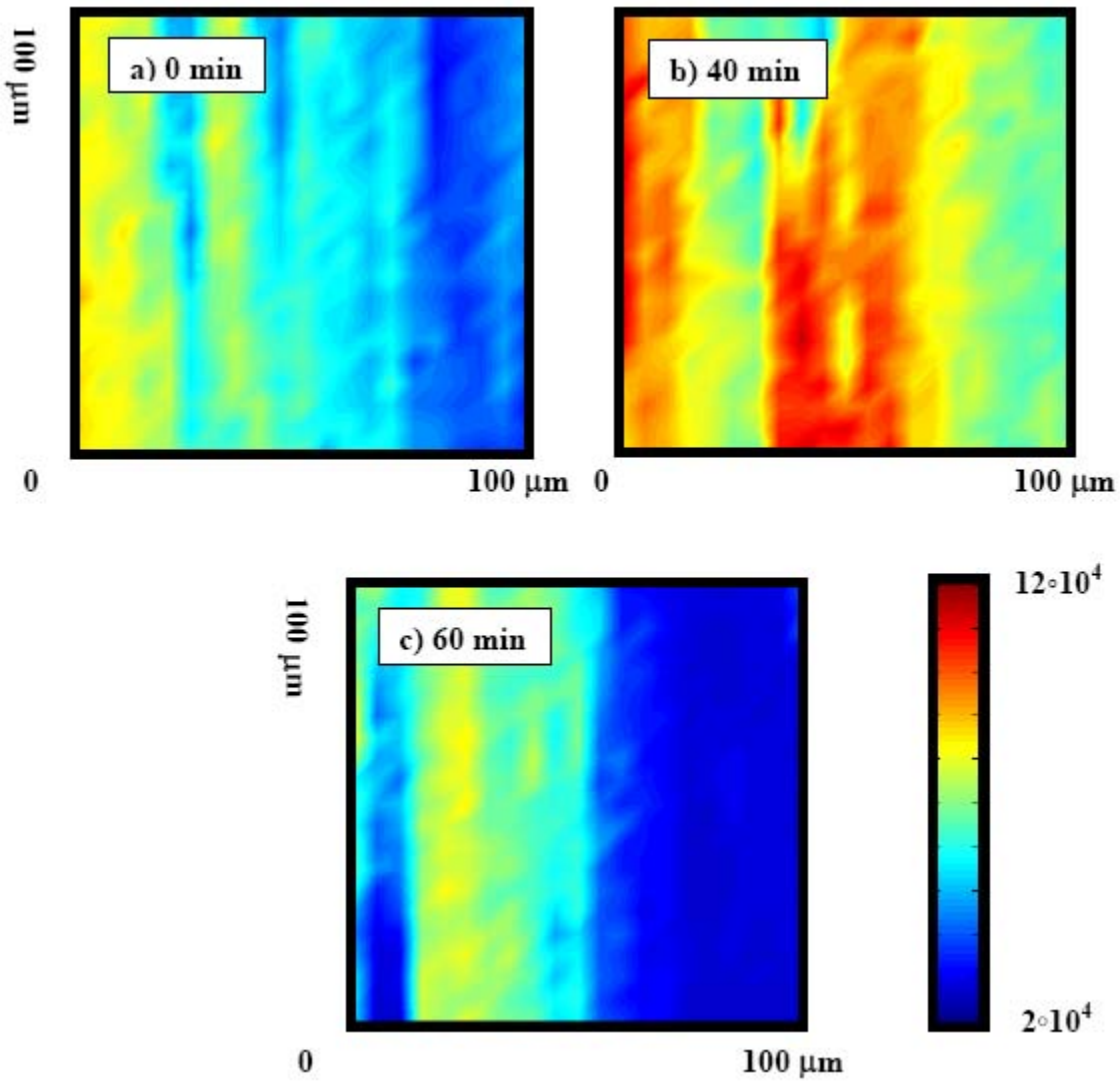

Fig.7. Variation of quality factor over surface area of 100 µm x 100 µm for Si-face (3 h) CNT film as grown (a) and after 40 min (b) and 60 min (c) annealing time in oxygen at 400°C.

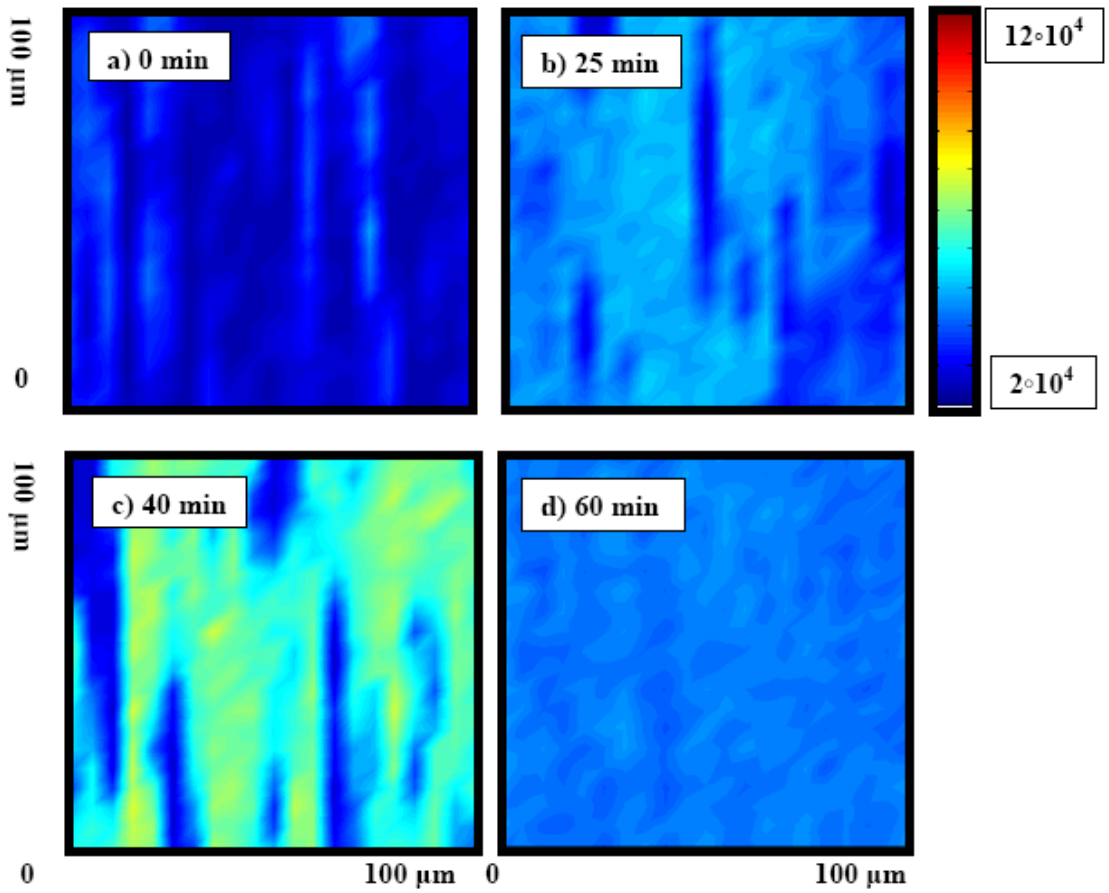

Fig.8. Variation of quality factor over surface area of 100 µm x 100 µm for Si-face (6 h) CNT film as grown (a) and after 25 min (a), 40 min (c) and 60 min (d) annealing time in carbon dioxide at 400°C.

THEORETICAL BACKGROUND

The extraction of data through evanescent microwave microscopy requires detailed knowledge of the field configuration outside the probe-tip region. The resonator tip is represented as a charged conducting sphere with a given potential: when placed in close proximity to a sample, the material is polarized by the electric field. The dielectric response to the tip causes a redistribution of charge on the tip in order to maintain the equipotential surface of the sphere, and also results in a shift in the frequency of the resonator. Applying the method of images, the field distribution requires a series of three

image charges in an iterative process to meet the boundary conditions at the probe tip and the dielectric sample surface (see details in [29]).

The theory applied for the microwave resonator deals only with the field distributed outside the tip including a sample space. The fundamental assumption of the theory is that the presence of the material introduces a perturbation to the existing electromagnetic field distribution. The changes in resonant frequency and reciprocal quality factor are described by Eqs.(1)-(3) [30]-[31]:

$$-2\frac{\Delta f}{f}-i\Delta\left(\frac{1}{Q}\right)=\frac{\int_V(\Delta\varepsilon\vec{E}_0^*\circ\vec{E}+\Delta\mu\vec{H}_0^*\circ\vec{H})dV}{\int_V(\varepsilon\vec{E}_0^*\circ\vec{E}+\mu\vec{H}_0^*\circ\vec{H})dV} \tag{1}$$

$$\frac{\Delta f}{f}=\frac{(f-f_0)}{f} \tag{2}$$

$$\Delta\left(\frac{1}{Q}\right)=\frac{1}{Q}-\frac{1}{Q_0} \tag{3}$$

where $\vec{E}_0$ and $\vec{H}_0$ are the unperturbed electric and magnetic fields, $\vec{E}$ and $\vec{H}$ are the perturbed fields, V is the volume of a region outside the resonator tip, f and Q are the perturbed resonant frequency and quality factor and f_0 and Q_0 are the reference (or unperturbed) resonant frequency and quality factor, respectively.

The right hand side of Eq.(1) is a complex number dependent on the local complex permittivity, describing dielectric and conductive properties of the materials. Although this can be solved for the general case, let us restrict our discussion to the case when the tip touches the sample (g is the distance between a tip and a sample).

$$\frac{\Delta f}{f(g=0)}=\frac{f(g=0)-f_0}{f(g=0)}=\frac{1}{2}\mathrm{Re}\left[1+\frac{\ln(1-b)}{b}\right]\ , \tag{4}$$

$$\Delta\left(\frac{1}{Q}\right)=\frac{1}{Q(g=0)}-\frac{1}{Q_0}=\mathrm{Im}\left[1+\frac{\ln(1-b)}{b}\right]. \qquad (5)$$

These two Eqs.(4) and (5) may be rearranged into more appropriate forms assuming that we know experimentally f_0 and Q_0:

$$f(g=0)=\frac{f_0}{\left[1+\frac{1}{2}\mathrm{Re}\left(\frac{b}{2}+\frac{b^2}{3}+...\right)\right]}, \qquad (6)$$

$$Q(g=0)=\frac{Q_0}{\left[1-Q_0\,\mathrm{Im}\left(\frac{b}{2}+\frac{b^2}{3}+...\right)\right]}, \qquad (7)$$

and

$$b=\frac{\varepsilon_1-1-i\varepsilon_2}{\varepsilon_1+1-i\varepsilon_2},\varepsilon_2=\frac{\varepsilon''}{\varepsilon_0}(=\frac{\sigma}{\omega\varepsilon_0}),\varepsilon_1=\frac{\varepsilon'}{\varepsilon_0}. \qquad (8)$$

By using Eq.(8), the approximate expression for the perturbed resonant frequency and quality factor at g = 0 have the forms given in Eqs.(9) and (10), respectively:

$$f(g=0)=\frac{f_0}{1-\frac{1}{2}-\frac{x\ln\sqrt{(1-x)^2+y^2}-y\arctan\frac{y}{(1-x)}}{2(x^2+y^2)}}, \qquad (9)$$

$$Q(g=0)=\frac{Q_0}{1+Q_0\dfrac{x\arctan\dfrac{y}{(1-x)}+y\ln\sqrt{(1-x)^2+y^2}}{x^2+y^2}}\,, \qquad (10)$$

where

$$x=\frac{\alpha}{\beta},\ y=\frac{2\varepsilon_2}{\beta}\,, \qquad (11)$$

$$\alpha=\varepsilon_1{}^2+\varepsilon_2{}^2-1,\beta=(\varepsilon_1+1)^2+\varepsilon_2{}^2.$$

RESULTS AND DISCUSSION

When the resonator tip approaches the surface of the sample, the resonant frequency f and quality factor Q will change. In measuring the frequency shift and the quality factor, the reference resonant frequency f_0 and corresponding Q_0 are set at a significant distance above the sample (theoretically at infinity). This distance between the probe tip and the sample should be sufficient to make sure that evanescent field from the tip is not interacting with the sample. Typical experimental data for the resonant frequency and quality factor were collected (Si-face, 3 h) for a sample-tip distance (g) between 1 μm and 10 μm (see Figs. 5 and 6). However, the resonant frequency f and the Q-factor cannot be measured when the tip touches the sample since it will damage the tip. In order to use Eq.(9) and Eq.(10) for calculation of real and imaginary parts of permittivity we need the value for f and Q at g = 0. The approach which has been used here to find these values is to approximate existing experimental data by exponential functions, allowing us to find reference values for f_0 and Q_0 and their respective values at g = 0. It appears that the empirical exponential forms in Eqs.(12) and (13) perfectly match the experimental data (Figs.5 and 6):

$$f=(-5.753\cdot10^{-5}\cdot e^{-0.376g}+1.1369)\text{GHz}=f(g)\,, \qquad (12)$$

$$1/Q = 1.470 \cdot 10^{-5} \cdot e^{-0.388g} + 2.269 \cdot 10^{-5} = 1/Q(g) \ , \qquad (13)$$

giving the values for f and Q in Eq.(14):

$$\begin{aligned} &f_0 = 1.1369\,\text{GHz}, 1/Q_0 = 2.269 \cdot 10^{-5}, f(g=0) = 1.1368\,\text{GHz}, \\ &1/Q(g=0) = 3.739 \cdot 10^{-5}. \end{aligned} \qquad (14)$$

The changes in resonant frequency and quality factor between these two extreme positions therefore amount to:

$$\begin{aligned} &\frac{\Delta f}{f(g=0)} = \frac{f(g=0) - f_0}{f(g=0)} = -5.061 \cdot 10^{-5}, \\ &\Delta\left(\frac{1}{Q}\right) = \frac{1}{Q(g=0)} - \frac{1}{Q_0} = 1.470 \cdot 10^{-5}. \end{aligned} \qquad (15)$$

Eqs.(16) and (17) can be obtained from Eqs.(9) and (10):

$$\frac{2(\Delta f)}{A \cdot f(g=0)} = 1 + \frac{x\ln\sqrt{(1-x)^2 + y^2} - y\arctan\dfrac{y}{(1-x)}}{(x^2 + y^2)} \ , \qquad (16)$$

$$\left(\frac{1}{B}\right)\Delta\left(\frac{1}{Q}\right) = \frac{x\arctan\dfrac{y}{(1-x)} + y\ln\sqrt{(1-x)^2 + y^2}}{x^2 + y^2} \ . \qquad (17)$$

Substituting the values from Eq.(15), and the values $B = 4.12 \cdot 10^{-5}$ and $A = 1.738 \cdot 10^{-4}$ determined experimentally [26], we can solve Eqs.(16) and (17) with respect to x and y. By using Eq.(11) we finally arrive at the effective values of complex permittivity listed in

Tab.IV for the CNT film (Si-face, 3 h) at ~1 GHz subjected to annealing in oxygen at 400°C for 40 min and 60 min. These values of ε_1 and ε_2 have been calculated from

TAB.IV. REAL (ε_1) AND IMAGINARY (ε_2) VALUE OF COMPLEX PERMITTIVITY FOR CNT FILM (Si-FACE, 3 h) AS GROWN AND AFTER 40 MIN AND 60 MIN OXYGEN TREATMENT AT 400°C.

ANNEALING TIME (min)	$\Delta(1/Q)$ (10^{-5})	$\Delta f/f(g=0)$ (10^{-5})	ε_1	ε_2
0	1.47	-5.06	3.83	2.85
40	2.45	-5.25	2.94	4.67
60	1.59	-9.22	18.05	9.52

Eqs.(16) and (17) by using the experimental values for $\Delta(1/Q)$ and $\Delta f/f(g=0)$ listed in Tab.IV.

This process described by Eqs.(12)-(17) is repeated for two other carbon nanotube samples grown for 3 h on Si-face and treated in the flowing oxygen for 40 min and 60 min. Tab.IV summarizes experimental data and theoretical results for ε_1 and ε_2 [32]-[33].

The experimentally determined frequency shift is the largest for the CNT film treated for 60 min in flowing oxygen. The reciprocal Q-factor change appears to have a maximum for the film subjected to annealing for 40 min: this quantity is related to local conductivity of the CNT film.

We have mapped several locations over an area of 100 μm x 100 μm by measuring the quality factor for each CNT film (see Fig.7). The mean Q-factor for each case was calculated and the values are summarized in Tab.V.

TAB.V. MEAN Q-FACTOR FOR AS GROWN AND TREATED Si-FACE (3 h) CNT FILMS IN FLOWING OXYGEN.

CNT FILMS (Si-FACE, 3 h)	MEAN Q-FACTOR ($\times 10^4$ arb.units)
AS GROWN	5.86
40 min	8.31
60 min	4.82

Fig.8 shows Q-factor mapping over several locations of an area 100 μm x 100 μm on a Si-face (6 h) CNT film as grown and after 25 min, 40 min and 60 min of annealing under carbon dioxide flowing gas. The mean Q-factor for each case was calculated and the values are summarized in Tab.VI.

TAB.VI. MEAN Q-FACTOR FOR AS GROWN AND TREATED Si-FACE (6 h) CNT FILMS IN FLOWING CARBON DIOXIDE.

CNT FILMS (Si-FACE, 6 h)	MEAN Q-FACTOR ($\times 10^4$ arb.units)
AS GROWN	2.92
25 min	4.37
40 min	5.71
60 min	4.33

From the conductivity maps and the data recorded in the Tabs.V-VI, it is clear that the overall surface conductivity of the sample reaches a maximum after 40 minutes of annealing independent of the type of gas used. The mean conductivity increases 34.2% after 25 min and 41.8 % after 40 min of annealing for the CNT film (Si-face, 3 h). This is due to the annealing treatment which removes the amorphous carbon layer and adsorbed molecules from the surface of carbon nanotubes. However, after 60 min of annealing, there is a 41.9 % decrease in the conductivity. This is because, after 60 min carbon nanotubes are already uncapped (see Fig.4) and due to oxidation of the tube tips they start to be more dielectric, which lowers the overall conductivity of the CNT film. The same behavior was observed in other CNT films including these treated in flowing carbon dioxide. The percentage of change was slightly higher in the film treated with carbon dioxide.

CONCLUSION

The surface conductivity plots show that the conductivity of the CNT films improved after 25 min and reached a maximum after 40 min of annealing. This is because the annealing treatment removes the amorphous carbon and the adsorbed molecules from the surface of the CNT film. These results have been confirmed by the AFM analysis (see Fig.4). The clean CNT films have a higher conductivity which explains the increase in the Q-factor after the annealing treatment. However, after 60 min, the conductivity decreases as the carbon nanotubes appear to be opened and these oxidized and open tips result in the lower conductivity of the CNT film. The shift of the reciprocal Q-factor between g = 0 and infinity is in agreement with the experimental data i.e., the shift in the reciprocal of the quality factor is greater for the most conductive CNT film.

In summary, it is important to stress that CNT films fabricated by thermal decomposition of SiC did not show significant percolative behavior based on evanescent

microwave measurements or spectroscopic ellipsometry [29,32]. This could be due to the presence of amorphous carbon in the system, occupying space between carbon nanotubes and on the surface of the CNT films and/or due to a majority of single- or multi-walled carbon nanotubes being semiconducting. The treatment of CNT films in oxygen or in carbon dioxide in 40 min time removes amorphous carbon at least from the film surface causing an increase in surface conductivity. If the oxidation time is longer then 40 min apparently the presence of open tips of nanotubes results in a decrease of the CNT film surface conductivity. This maximum in the quality factor due to mapping (Tabs.IV-V) or the maximum in the total change in the reciprocal of the quality factor (Fig.6) can be an indicator of the beginning of the uncapping process of the carbon nanotubes. Depending on the storage (uncapped CNTs) or emission (capped CNTs) application we can use this maximum as a divider between these two applications assuming that the film is already purified from amorphous carbon. The two-point theoretical model [29] has established very simple relationships between the complex permittivity and both the relative resonant frequency shift of the resonator $\Delta f/f(g = 0)$ and the reciprocal change of quality factor $\Delta(1/Q)$ which have been experimentally measured. The values of the real and imaginary parts of the complex permittivity in CNT films are amongst the other important results coming from the model.

REFERENCES

[1] Iijima S 1991 *Nature (London)* **354** 56

[2] Dresselhaus M S, Dresselhaus G and Eklund P C 1996 *Science of fullerenes and carbon nanotubes* Academic Press New York

[3] Wildoer J W G et al. 1998 *Nature* **391** 59

[4] Odom T W, Huang J L, Kim P and Lieber C M 1998 *Nature* **391** 62

[5] Falvo M R et al. 1997 *Nature* **389** 582

[6] Dai H et al. 1996 *Nature* **384** 147

[7] de Heer W A, Châtelain A and Ugarte D 1995 *Science* **270** 1179

[8] Rinzler A G et al. 1995 *Science* **269** 1550

[9] Collins P G and Zettl A 1996 *Appl. Phys. Lett.* **69** 1969

[10] Bonard J M et al. 1998 *Ultramicroscopy* **73** 7

[11] Wang Q H et al. 1997 *Appl. Phys. Lett.* **70** 3308

[12] Kariyawasam T *Field Emission of Carbon Nanotubes,* http://www.physics.uc.edu/~jarrell/COURSES/ELECTRODYNAMICS/Student_ Projects/tharanga/review.pdf

[13] Bonard J M, Salvetat J P, Stockli T, Forro L and Chatelain A 1999 *Appl.Phys.A* **69** 245

[14] Seelaboyina R and Choi W B 2007 *Recent Patent on Nanotechnology* **1** 238

[15] Seelaboyina R, Boddepalli S, Noh K S, Joen M H and Choi W B 2008 *Nanotechnology* **19** 1

[16] Chen S Y, Miao H Y, Lue J T and Ouyang M S 2004 *J.Phys.D:Appl.Phys.* **37** 273

[17] Liu Y M and Fan S S 2005 *Solid State Commun.* **133** 131

[18] Nilsson L, Groening O, Emmenegger C, Kuettel O, Schaller E, Schlapbach L, Kind H, Bonard J M and Kern K 2000 *Appl.Phys.Lett.* **76** 2071

[19] Kusunoki M, Suzuki T, Kaneko K and Itos M 1999 *Phil. Mag. Lett.* **79** 153

[20] Kusunoki M, Suzuki T, Hirayama T and Shibata N 2000 *Appl.Phys.Lett.* **77** 531

[21] Mitchel W C, Boeckl J J, Toln D, Lu W, Rigueur J and Reynolds J 2005 *Quantum sensing and nanophotonic devices II, Proceedings of the SPIE* **5732** 77

[22] Ajayan P M, Ebbesen T W, Ichihashi T, Iijima S, Tanigaki K and Hiura H 1993 *Nature* **362** 522

[23] Tsang S C, Harris P J F and Green M L H 1993 *Nature* **362** 520

[24] Biro L P, Bernardo C A, Tibbetts G G and Lambin Ph *Carbon Filaments and Nanotubes: Common Origins, Differing Applications?* Springer Verlag 2001, Series E: Applied Sciences **372**

[25] Geng H Z, Zhang X B, Mao S H, Kleinhammes A, Shimoda H, Wu Y and Zhou O 2004 *Chem.Phys.Lett.* **399** 109

[26] Kleismit R A, ElAshry M, Kozlowski G, Amer M S, Kazimierczuk M K and Biggers R R 2005 *Supercond.Sci.Technol.* **18** 1197

[27] Xiang X D and Gao C 2002 *Mater.Character.* **48** 117

[28] Boeckl J J, Mitchel W C, Rigeur J and Lu W 2005 *Proceedings of International Conference on SiC and Related Materials* 1579

[29] Kozlowski G, Kleismit R A, Boeckl J J, Campbell A L, Munbodh K, Hopkins S C, Koziol K K and Peterson T L 2008 *Nanotechnology*

[30] Li D Q, Free C E, Pitt K E G and Barnwell P G 2001 *IEEE Microwave and Wireless Components Lett.* **11** 118

[31] Sucher M and Fox J 1963 *Handbook of Microwave Measurements* Brooklyn NY Brooklyn Polytechnic Inst. Press, Vol.II

[32] Harrison J, Sambandam S N, Boeckl J J, Mitchel W C, Collins W E and Lu W J 2007 *J.Appl.Phys.* **101** 104311

[33] Fagan J A, Simpson J R, Landi B J, Richter L J, Mandelbaum I, Bajpai V, Ho D L, Raffaelle R., Hight Walker A R, Bauer B J and Hobbie E K 2007 *Phys.Rev.Lett.* **98** 147402-1